SCIENTIFIC PRESENTATION GUIDELINES

Dr. Fern Tsien
Department of Genetics
LSUHSC

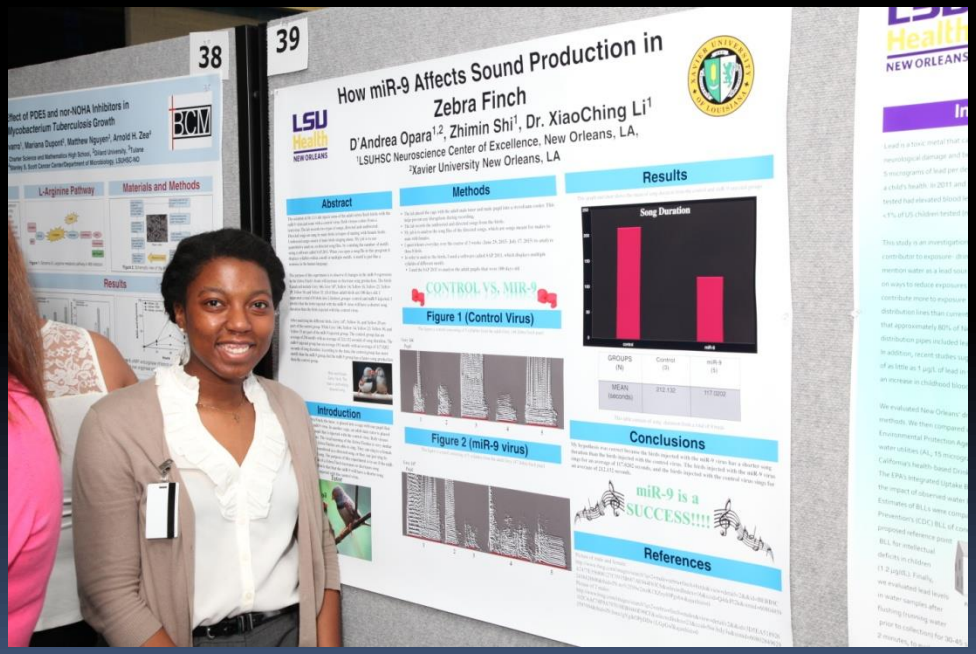

Important Deadline #1: Abstracts

- Abstracts are due on or before Thursday, July 20th by 2:00 pm!!!
- Medical student abstracts are due on August 1st .
- Follow the guidelines sent to you.
- DO NOT change the margins, font size, or font style.
- We will use the abstract you send us to generate the Abstract Book to give out during the poster session and to the judges ahead of time.

What is an Abstract?

- An abstract is a one-page summary of your project.
- List your name and mentor's name as described in the template.
- Affiliations: department and school.
- Use only the template we provide.
- This template has the correct sized fonts and sizes we will use. Do not change the font or size!
- Follow the directions provided by Ms. Angel Loveless.
- Make sure your mentor approves of your abstract before you send it to us!
- When you submit your abstract in Word format, please be sure to save the file with your last name listed first. For example: LovelessAngelAbstract.doc
- Send it to: to Ms. Angel Loveless **alove1@lsuhsc.edu** **and** Noel Netzhammer **nnetzh@lsuhsc.edu**

Your Name (first, middle initial, last)
Classification (High School, Undergraduate, Medical)
Name of School, City, State

Mentor's Name:
Mentor's Affiliation (LSUHSC, Tulane SOM, Xavier, Children's Hospital, etc.)

"Title of Project"

Abstract (summary of project, not to exceed one page)

Body of Abstract: Left Justified, 11 pt Arial font.

Jonathan, S, Lee
Undergraduate
Case Western Reserve University, Cleveland, Ohio

Mentor: Ashok Aiyar, Ph.D
Louisiana State University Health Sciences Center, Department of Microbiology, Immunology & Parasitology

"The effect of high-risk HPV E6 & E7 oncogenes on the STD bacterium *Chlamydia trachomatis*"

Chlamydia trachomatis is an obligate intracellular bacterium that infects human epithelial cells. *Chlamydia trachomatis* causes the most widely reported case of sexually transmitted infections in the United States, with an estimate of 2.86 million infections occurring annually. In addition, chlamydial infections of conjunctival epithelial cells are the world's leading cause of infectious blindness. Studies examining the cellular pathology caused by *C. trachomatis* have largely relied n human epithelial cell-lines, such as the cervical cancer cell-line Hela (and its derivates – Hep-2, KB, etc.). All of these cell-lines are transformed by high-risk human papillomaviruses (HPV) and express the E6 and E7 oncogenes of these viruses. It has been recently shown that the effect of the protective cytokine, IFNγ, on *Chlamydia* replication is cell-line dependent. IFNγ protects against chlamydial infections by inducing cellular enzymes that deplete the amino-acid tryptophan, which is essential for chlamydial growth and development.

From previous experiments, it has been observed that the capacity of IFNγ to block chlamydial replication is significantly more pronounced when tested using HPV E6/E7-expressing cells than HPV-negative cells. It has been reported in the literature that the expression of several proteasomal subunits is lower in HPV-positive cell-lines. We believe that the reduced proteasomal activity in such cells decreases the intracellular pool of tryptophan generated by protein recycling/degradation during amino-acid starvation. Thus, the decreased intracellular free amino-acid pools in HPV-positive cells accentuate the effect of IFNγ on Chlamydia. We have tested this hypothesis by making derivates of HPV-negative cell-lines to express the E6 and E7 oncogenes of HPV. Chlamydial replication is severely reduced in the E6/E7-expressing derivative cell-lines relative to the parental HPV-negative cells during amino-acid starvation. We are currently examining the expression of proteasomal subunits by immunoblotting these cell-lines.

These effects of HPV oncogenes on *Chlamydia* make it desirable to construct immortalized cell-lines without using E6 & E7 to study chlamydial biology. We have constructed retroviral vectors to facilitate this, and will describe their design and construction.

What is wrong with this abstract?

Mechanisms Underlying the Sleep Promoting Effect of Cherry Juice Standardized to its Proanthocyanidin Content

Previous studies have shown that tryptophan, melatonin, and proanthocyanidin within cherry juice may play essential roles in promoting sleep. This study utilizes cherry juice standardized to its proanthocyanidin content and tests its effectiveness as a treatment for insomnia, a common health problem in the elderly. Ten participants with insomnia complete two treatment periods (cherry juice and placebo juice), 2 weeks each, separated by a 2 week washout period. Each day the participants consume 8 ounces of juice in the morning and again 1-2 hours before bedtime. Overnight polysomnography (PSG) is used at the end of each treatment period to evaluate sleep architecture such as the distribution of sleep stages, sleep latency and state transitions. Blood samples are also taken to measure serum concentrations of free tryptophan and kynurenine in order to investigate a possible mechanism of action. Questionnaires are given before and after each two week treatment period for comparison of each treatment's effects. This study is still ongoing and data analysis will be performed upon its completion.

Important Deadline #2:

- Posters are due Monday, July 24th, 2017 at 2:00 pm!

If we do not receive a poster by this date, your mentor will be responsible for the printing of the poster!!!

Important deadline #3:

Summer Research Internship Poster Day
Thursday, July 27th, 2017

- 1st floor lobby of Medical Education Building (MEB), Lecture Room B, 1900 Perdido St., NO, LA 70112

8:00 am-9:00 am	Put up your poster
9:00 am-10:00 am	Interns and judges only
10:00 am-11:00 am	Open to the public
11:00 am- 12:00 noon	Awards ceremony, open to the public in MEB Lecture Room B

Who will be presenting posters?

- All high school and undergraduates in this program are required to present a poster on July 27th .
- Since classes begin early for medical students, they will present their posters during the medical research day in the fall.
- Student presentations will be judged and awards will be given for each category.

Preparing the posters 1

- First and most important: make sure that your mentor approves of the information that will be presented in the poster.
- Second most important: Your name should go first, your mentor's name last, and everyone else who helped you (other students, post-docs, etc.) in the middle. Make sure not to leave out anyone who helped you!
- Make sure that you understand everything you write on the poster. You should be able to explain your project to the judges.
- In general, try to keep text towards the outside and figures and tables in the center.
- The abstract is not necessary for the poster.

Preparing the posters 2

- Use the Power Point poster template sent to you by Ms. Angel Loveless(not your friend's or past interns) with the proper logos.
- These correspond to your mentor's affiliation and the Summer Program funding source.
- The logos on your poster may differ from the ones on your lab mates! Do not change them!
- Use at least a 24 point font size so the text will be visible from 3 feet away.
- Feel free to adjust the box sizes and headings depending on the amount of text or figures you have.
- The poster template are already set to 34 x 44 inches.

Preparing the posters 3

- Use any color you want to. Express yourself! Exceptions:
  - Black or deep blue for background of entire poster.
  - Image enlarged to cover the entire background.
- Spell out any acronyms the first time you use them. People outside of your lab do not know what "DBS" or "FSHD" is.
- Refer to guidelines sent to you.

Once your poster is done:

- Save it as a PPT and PDF file.
- When you submit your poster, be sure to save the file with your last name listed first. For example: LovelessAngelPoster.pptx
- Send it to: Send it to: to Ms. Angel Loveless **alove1@lsuhsc.edu** **and** Noel Netzhammer **nnetzh@lsuhsc.edu**
- You will be notified when your poster is ready to pick up from the Genetics office.
- You are responsible for hanging up the poster on July 27th .
- Plan to take your poster down at the end of the poster session and give it to your mentor. Let us know in advance if you want an extra one for your school.
- Posters are due July 24th !!!
- If we do not receive a poster by this date, your mentor will be responsible for the printing of the poster.

Next: Practice your presentation

- Practice with your mentor and your lab members!
- Anticipate questions and look up the answers ahead of time
- Practice, practice, practice so you sound polished.
- Practice in front of your friends or in front of a mirror.

What happens at a poster session?

- Please dress appropriately (business attire).
- The posters will be displayed early so the judges will have a chance to see them ahead of time. Also, they will have a copy of the abstracts.
- Stand by your poster. Judges will be passing by asking you questions.
- The posters will be judged on poster display and your presentation (enthusiasm, understanding of the topic, etc)
- Practice ahead of time a short (2-5 minute) description of your poster. Sometimes people ask specific questions, sometimes they ask "tell me about your project"
- DO NOT READ THE POSTER TO THE JUDGES
- Think of possible questions you may be asked. If you do not know an answer, it is OK to say "I don't know"
- After the judging, the posters will be available to the public. Your family is invited.
- Then we will move to the MEB Lecture Room B on the 1st floor and give out awards!

What happens at a poster session?

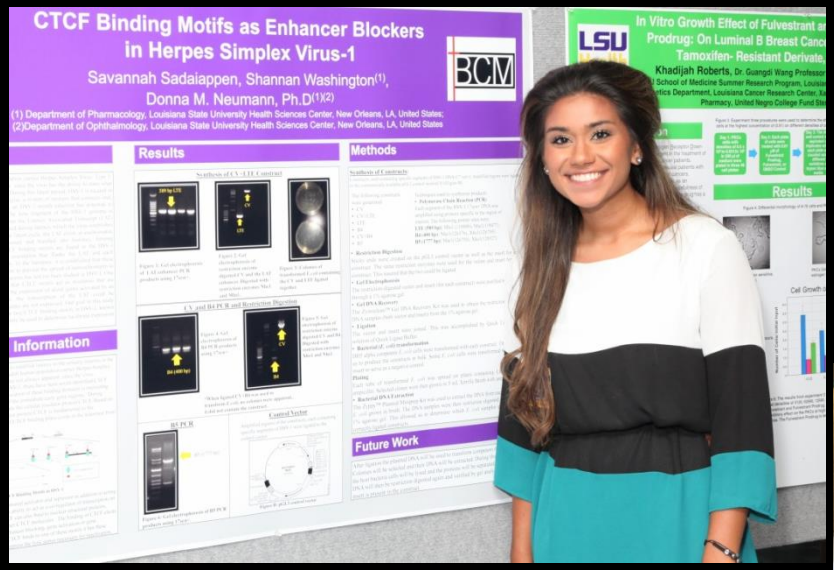

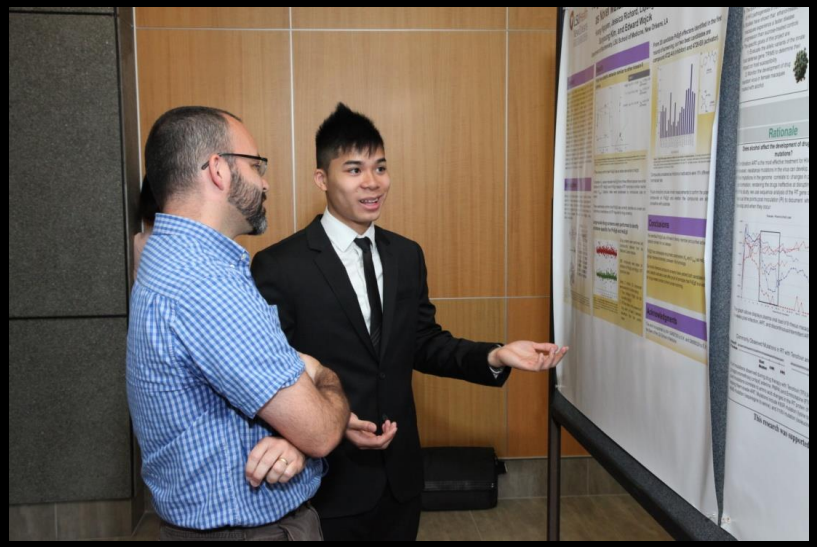

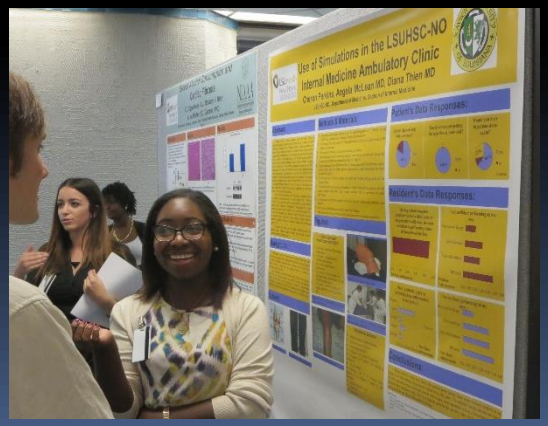

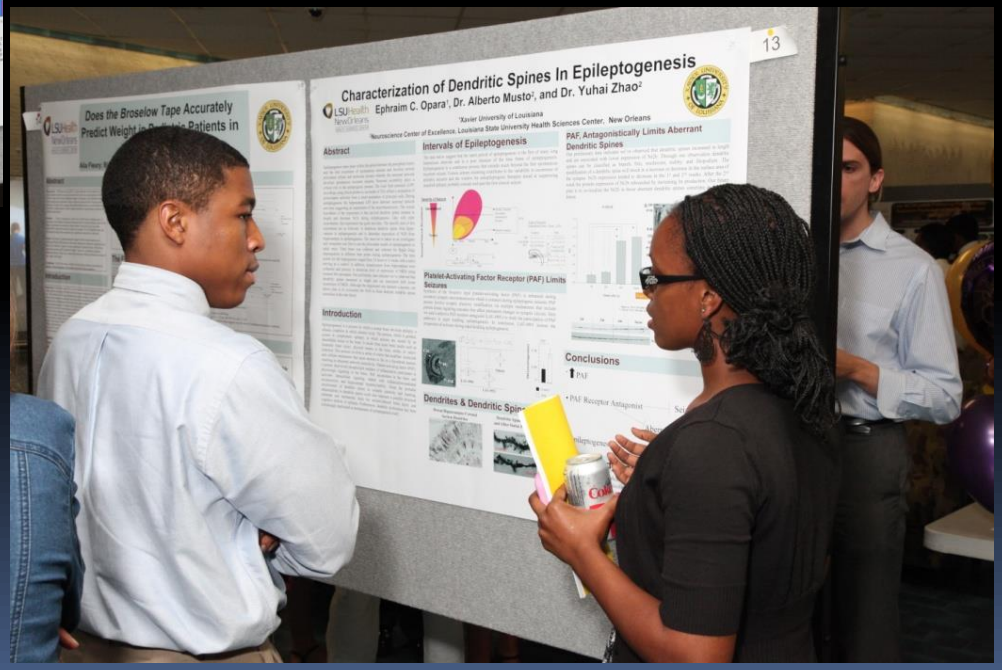


44
CBA Dysregulates Mesenteric Adipose Tissue Phenotype in SIV-Infected Macaques
Joshua Ricks, Curtis Vande Slouwe, Paul Berner, Liz Simon, and Patricia E Molina
Department of Physiology, Louisiana State University Health Sciences Center, New Orleans
NIH

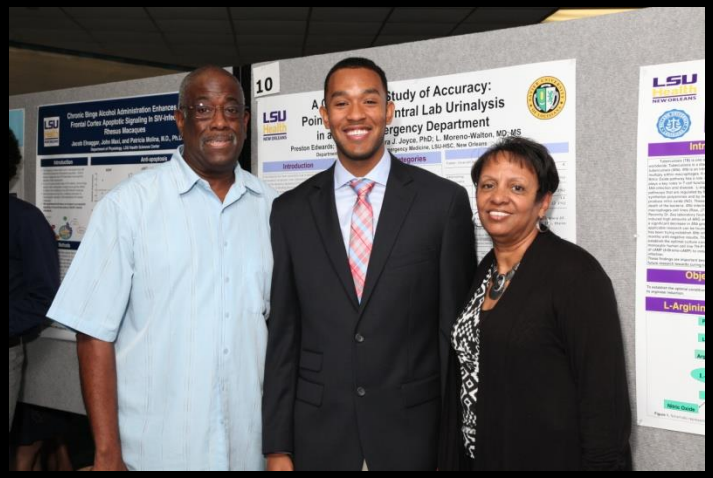
10
Study of Accuracy:
Central Lab Urinalysis
Emergency Department
LSU


LSUHealth NewOrleans
Assessment of Need for Targeted Acute HIV Testing
Chante Jones; Benjamin I. Lee, MPH; Erin Simmons, MD, MPH; Lisa Moreno-Walton, MD, MS, MSCR
Section of Emergency Medicine, Louisiana State University Health Sciences Center
Introduction
Cohort Description
Results
Conclusions
Discussion
Acknowledgments
A New Purpose for an Old Drug: Inhibiting Autophagy with 3-Methyladenine in Ataxia Telangiectasia
Eric Lorie; Ryan Reed

Nervousness: How to fight back

- Practice ahead of time. A well organized, practiced talk will almost always go well.
- If you draw a blank, then looking at your poster will help you get back on track.
- Taking a deep breath will calm you down.
- Slow down. Take a few seconds to think about a question that is being asked before you answer it.
- Bring notes. if you are afraid that you will forget a point, write it down on a piece of paper and bring it with you. However, you don't want to have a verbatim copy of your talk, instead write down key phrases that you want to remember to say.

Nervousness: How to fight back

- Be prepared to answer questions. You don't have to know the answer to every question, however you should be prepared to answer questions about your work. Before the poster session, think about what questions you are likely to get, and how you would answer them
- It is okay to say "I don't know" or “I hadn't thought about that, but one possible approach would be to…"

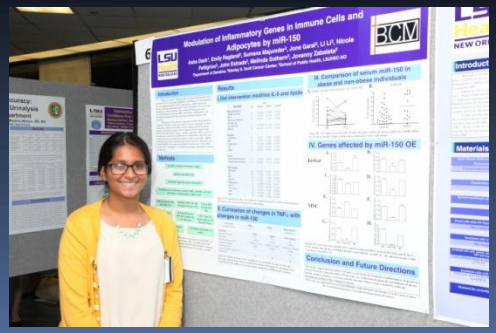

What is wrong with this poster?

PATRICK F. TAYLOR FOUNDATION

Effect of Gain-of-Function Mutant Rb on the Sphere-Forming Ability of Cell Lines

Your name goes first, Graduate students and post-docs that helped you, Mentor is last

Mentor's department and University

LSU Health Sciences Center

Abstract

Osteosarcoma, the most common bone cancer, is the second highest cause of cancer-related death in children and adolescents. Approximately 90% of cases show micro-metastasis at diagnosis, making systematic chemotherapy the first choice of treatment. Despite intensive chemotherapy, the survival rate for high-grade osteosarcomas remains at only 50-80%. This persistence is mainly due to the ability of osteosarcoma cells to metastasize and develop resistance to therapy. Increasing evidence suggests that cancer stem cells (CSCs) or tumor initiating cells (TICs) are responsible for these properties and that the inadequacy of current treatments may be result from the inability to target CSCs or TICs in osteosarcoma. Recently, we have demonstrated that small populations of osteosarcoma cells can grow and form spheres in both serum- and anchorage-independent manners. Importantly, as few as 200 cells from these spheres efficiently initiated osteosarcomas in tumor transplantation models. These results suggest that spheres are enriched with osteosarcoma CSCs. Approximately 50% of osteosarcomas contain alterations in the tumor suppressor *p53* gene. Many hotspot p53 mutants show oncogenic functions by their gain-of-function phenotypes such as increased transformation, metastasis and drug resistance, which can not be explained simply due to loss of wild-type p53 function. Our preliminary results indicate that downregulation of a gain-of-function mutant p53R172H results in a dramatic reduction of sphere-forming ability of an osteosarcoma cell line expressing p53R172H. These results suggest that mutant p53 gain-of-function is involved in sphere-forming ability and possibly CSC-like properties of osteosarcoma. However, the exact molecular mechanisms which contribute to sphere formation and CSC-like properties and the involvement of mutant p53 in these cellular phenotypes remain unclear.

Our long-term goal is to identify the molecular mechanism underlying the CSC-like properties of osteosarcoma. *The objective of this study* is to investigate the effects of several hotspot p53 mutants on the sphere-forming ability of human osteosarcoma cell lines. *Our hypothesis is that gain-of-function p53 mutants increase the sphere-forming ability of osteosarcoma cells.* To test our hypothesis, we first characterized the sphere-forming ability of several available human osteosarcoma cell lines, such as U2OS (p53 wild-type), SJSA1 (p53 wild-type), MG63 (p53-null), Saos-2 (p53-null), and KHOS (p53R156P). We found that U2OS and MG63 cell lines did not show any sphere formation when 500 cells were tested for 2 weeks of culturing in sphere-specific conditions. These results may suggest that the presence of wild-type p53 is not crucial for the sphere formation. Assays for other cell lines are on-going. We next infected MG63 cells with retroviral vectors encoding p53R175H/72P, p53R175H/72R, p53R248W/72P, p53R248W/72R, p53R273H/72P, and p53R273H/72R to establish MG63 subcell lines expressing several gain-of-function p53 mutants together with different p53 codon 72 single nucleotide polymorphisms (SNPs), since the SNP is shown to affect colony-forming ability of human cancer cell lines. Sphere formation assays using these subcell lines are underway and all results will be presented. Completion of our study will provide a better understanding of the role of gain-of-function mutant p53 in sphere-forming ability of osteosarcoma as well as useful information to dissect the molecular mechanism of CSC-like properties of osteosarcoma.

Introduction

Osteosarcoma is a devastating disease in children and young adults. In approximately 90% of osteosarcoma cases, micro-metastases are present during diagnosis, making chemotherapy the first choice of treatment. Despite intensive chemotherapy, the survival rate for high-grade osteosarcomas remains at only 50-80%. This persistence is mainly due to the ability of osteosarcoma cells to metastasize and develop resistance to therapy. Increasing evidence suggests that cancer stem cells (CSCs) or tumor initiating cells (TICs) are responsible for the metastatic and drug-resistant properties of cancer cells and that the inadequacy of current treatments for high grade osteosarcoma may result from the inability to target osteosarcoma CSCs. CSCs represent a small fraction of a tumor's cellular population and have the ability to generate new tumors identical in cellular composition to the tumor of origin. CSCs possess the abilities of anchorage-independent, serum-independent cell growth (sphere formation), tumor initiation, self-renewability, and multilineage differentiation, as well as properties of high metastatic potential and drug resistance. We have recently reported that small number of osteosarcoma cells form spheres and these spheres are enriched with cells having CSC-like properties such as high metastatic and drug resistant properties. However, the molecular mechanism that regulates CSC-like properties of osteosarcoma remains unclear.

Cancer can arise through alterations to genes that regulate cell proliferation, apoptosis, and senescence. The tumor suppressor p53, one of the key guardians of these events, exerts its functions through transactivating numerous downstream targets. Tumor suppressor p53 has a single nucleotide polymorphism (SNP) at codon 72 which is either proline (P) or arginine (R). Recent studies have shown that the 72R form is more potent in its ability to induce apoptosis compared to the 72P form. In addition to the polymorphism, mutations in the *p53* gene affect the p53 activity. Mutations in the DNA binding domain attenuate the function of p53 as a transcription factor, thereby losing its tumor suppressor activity. The importance of p53 mutation is emphasized by the clinical observation that the *p53* gene is mutated in more than 50% of tumors. Mutations in the *p53* gene are also observed in approximately 70% of patients with Li-Fraumeni syndrome (LFS), a human familial cancer-prone disease. LFS is characterized by early onset of various types of tumors, including osteosarcoma. Several missense mutations such as R175H, R248W, and R273H, are the hotspot mutations in sporadic cancer as well as the germline of LFS patients. These p53 mutants show oncogenic functions by their gain-of-function phenotypes such as increased transformation, metastasis, and drug resistance, which can not be explained simply by loss of wild-type p53 function. The molecular mechanisms underlying the gain-of-function activities and if the codon 72 SNP affects the mutant p53's gain-of-function activities remain unclear. Further, although the gain-of-function phenotypes are similar to those of CSCs, the contributions of mutant p53 to the CSC-like properties are also unknown.

Methods and Materials

Cell lines. Human osteosarcoma cell lines U2OS, SJSA1, Saos-2, MG-63, and KHOS/NP were purchased from American Type Culture Collection (ATCC, Manassas, VA).

Sphere culture. Cells were counted by trypan-blue staining (Sigma Biochemicals), and live cells (five per well) were plated on a 96-well ultra-low attachment plate (Corning Inc., Corning, NY, USA) in sphere-specific media consisting of DMEM/F12, progesterone (10 nM), putrescine (50 μM), insulin (12.5 μg/ml), transferrin (12.5 μg/ml), sodium selenite (12.5 ng/ml, Sigma Biochemicals), murine EGF (10 ng/ml), and murine bFGF (10 ng/ml, Pepro Tech, Rocky Hill, NJ, USA). Cells were maintained for 10 – 14 days and fresh aliquots of EGF and bFGF were added three times a week. Sphere formation was observed daily using under a phase-contrast microscopy (Nikon Eclipse TS100).

Western blotting. MG-63 cells infected with retroviral vectors encoding control empty or a mutant p53 (R175H, R248W, or R273H) with a codon 72 polymorphism were lysed with RIPA buffer (50 mM Tris-HCl pH 7.6, 150 mM NaCl, 1 mM EDTA, 1% sodium deoxycholate, 0.1% Triton X-100, 0.1% SDS) supplemented with protease inhibitor cocktail (Roche) (1 mM phenylmethylsulfonyl fluoride (PMSF), 0.2 mM sodium orthovanadate, and 100 mM sodium fluorine). Whole cell extracts were separated by SDS-PAGE and transferred onto PVDF membranes (*GE Healthcare* Biosciences). After blocking with 5% non-fat milk in 1 x Tris-buffered saline (TBS) with 0.1% Tween-20 (TBS-T), blots were incubated with anti-human p53 (DO1, Santa Cruz) and control vinculin (Fitzgerald), followed by the incubation with secondary antibodies conjugated with horseradish peroxidase (Santa Cruz). To visualize signals, Super Signal West Dura Chemiluminescent substrates (Pierce Biotechnology) were used according to manufacture instructions. The signals were detected using a Biorad *Versa Doc* detection system (Biorad)

Sphere culture. Cells were counted by trypan-blue staining (Sigma Biochemicals), and live cells (five per well) were plated on a 96-well ultra-low attachment plate (Corning Inc., Corning, NY, USA) in sphere-specific media consisting of DMEM/F12, progesterone (10 nM), putrescine (50 μM), insulin (12.5 μg/ml), transferrin (12.5 μg/ml), sodium selenite (12.5 ng/ml, Sigma Biochemicals), murine EGF (10 ng/ml), and murine bFGF (10 ng/ml, Pepro Tech, Rocky Hill, NJ, USA). Cells were maintained for 10 – 14 days and fresh aliquots of EGF and bFGF were added three times a week. Sphere formation was observed daily using under a phase-contrast microscopy (Nikon Eclipse TS100).

Western blotting. MG-63 cells infected with retroviral vectors encoding control empty or a mutant p53 (R175H, R248W, or R273H) with a codon 72 polymorphism were lysed with RIPA buffer (50 mM Tris-HCl pH 7.6, 150 mM NaCl, 1 mM EDTA, 1% sodium deoxycholate, 0.1% Triton X-100, 0.1% SDS) supplemented with protease inhibitor cocktail (Roche) (1 mM phenylmethylsulfonyl fluoride (PMSF), 0.2 mM sodium orthovanadate, and 100 mM sodium fluorine). Whole cell extracts were separated by SDS-PAGE and transferred onto PVDF membranes (*GE Healthcare* Biosciences). After blocking with 5% non-fat milk in 1 x Tris-buffered saline (TBS) with 0.1% Tween-20 (TBS-T), blots were incubated with anti-human p53 (DO1, Santa Cruz) and control vinculin (Fitzgerald), followed by the incubation with secondary antibodies conjugated with horseradish peroxidase (Santa Cruz). To visualize signals, Super Signal West Dura Chemiluminescent substrates (Pierce Biotechnology) were used according to manufacture instructions. The signals were detected using a Biorad *Versa Doc* detection system (Biorad).

Figure 1

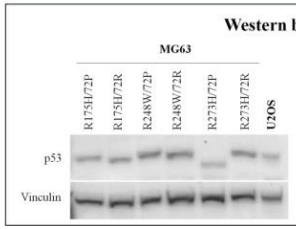

Figure 2. Western blotting. MG-63 cells were infected with mutant p53-encoding retroviral vectors to generate subcell lines expressing mutant p53. Cells were lysed in RIPA buffer and whole cell extracts were subjected to western blotting for p53 (DO1 antibody) and loading control vinculin. U2OS having wild-type p53 was used as a positive control.

Results

Our long-term goal is to identify the molecular mechanism underlying the CSC-like properties of osteosarcoma. *The objective of this study* is to investigate the effects of several hotspot p53 mutants on the sphere-forming ability of human osteosarcoma cell lines. *Our hypothesis is that gain-of-function p53 mutants increase the sphere-forming ability of osteosarcoma cells.* To test our hypothesis, we first characterized the sphere-forming ability of several available human osteosarcoma cell lines, such as U2OS (p53 wild-type), SJSA1 (p53 wild-type), MG63 (p53-null), Saos-2 (p53-null), and KHOS (p53R156P). We found that U2OS and MG63 cell lines did not show any sphere formation when 500 cells were tested for 2 weeks of culturing in sphere-specific conditions. These results may suggest that the presence of wild-type p53 is not crucial for the sphere formation. Assays for other cell lines are on-going. We next infected MG63 cells with retroviral vectors encoding p53R175H/72P, p53R175H/72R, p53R248W/72P, p53R248W/72R, p53R273H/72P, and p53R273H/72R to establish MG63 subcell lines expressing several gain-of-function p53 mutants together with different p53 codon 72 single nucleotide polymorphisms (SNPs), since the SNP is shown to affect colony-forming ability of human cancer cell lines. Sphere formation assays using these subcell lines are underway and all results will be presented. Completion of our study will provide a better understanding of the role of gain-of-function mutant p53 in sphere-forming ability of osteosarcoma as well as useful information to dissect the molecular mechanism of CSC-like properties of osteosarcoma.

Table 1

Table 1. Results of sphere formation assays

Cell lines	p53 status	Cell# examined	# of spheres formed	% sphere formation
U2OS	wild-type	480	0	0
SJSA1	wild-type	480	1	0
Saos-2	null	480	318	66.3
MG63	null	480	0	0
MG63 R175H/72P	R175H/72P	480	84	17.5
MG63 R175H/72R	R175H/72R	480	160	33.3
MG63 R248W/72P	R248W/72P	480	217	45.2
MG63 R248W/72R	R248W/72R	480	144	30.0
MG63 R273H/72P	R273H/72P	480	112	23.3
MG63 R273H/72R	R273H/72R	480	136	28.3
KHOS	R156P	480	112	23.3

Conclusions

Conclusions

1. Spheres vary in size and rate of growth in different osteosarcoma cell lines.
2. The presence or absence of wild-type p53 does not have any effects on the sphere-forming ability of osteosarcoma cell lines.
3. The presence of mutant p53 does enhance the sphere formation of osteosarcoma cells.
4. The effects of p53 codon 72 polymorphisms vary in different p53 mutations.
5. All p53 mutants confer osteosarcoma cells with sphere-forming abilities.

Future directions

1. Examine the effects of mutant p53 on other CSC-like properties such as tumor initiating ability, self-renewal, metastatic potential, and drug resistance.
2. Examine the effects of mutant p53 down-modulation in various osteosarcoma cell lines carrying mutant p53.
3. Identify genes that regulate sphere-forming ability and CSC-like properties of osteosarcoma cells.

Example of a better poster

RNA Binding ability of FUS mediates toxicity in a *Drosophila* model of ALS

Senthil S. Natarajan, J. Gavin Daigle, Nicholas A. Lanson, Jr., John Monaghan, Ian Casci, Udai B. Pandey

Department of Genetics, Louisiana State University Health Sciences Center, New Orleans, LA

LSU Health New Orleans HEALTH SCIENCES CENTER

LVC Louisiana Vaccine Center

Abstract

Amyotrophic Lateral Sclerosis (ALS) is a late-onset neurodegenerative disorder characterized by the loss of motor neurons. Mutations in Fused-in-Sarcoma (FUS) have been identified as a major component in both familial (FALS) and sporadic (SALS) ALS cases. FUS is an RNA-binding protein implicated in several processes like RNA splicing and microRNA processing. In normal individuals, the FUS gene is predominantly localized in the nucleus; however in ALS patients, FUS becomes redistributed to the cytoplasm as well, which is believed to be a causative pathway for ALS.

Ectopic expression of human FUS with ALS-linked mutations in fly eyes causes moderate to severe external eye degeneration. Here we examined the role of RNA binding in mediating the neurodegenerative effects of mutant FUS via the RNA Recognition Motif (RRM). The RRM domain in FUS is key to the RNA binding pathway and can be disrupted by total deletion of the domain itself (RRM-D) or by mutating 4 conserved phenylalanine residues within the FUS RRM to leucine (known as 4F-L). The 4F-L mutations have been previously shown to mitigate RNA binding ability in a yeast model of FUS.

We demonstrate that disrupting the RRM-Domain, by way of deletion or by the 4F-L point mutations, can suppress the toxicity of FUS. Interestingly, confocal imaging has shown that disrupting the RNA binding-ability keeps FUS within the nucleus (unlike in ALS cases, where FUS is redistributed to the cytoplasm), further indicating that subcellular mislocalization of FUS is a causative pathway for ALS.

In summary, we have identified a means of rescuing phenotype in our *Drosophila* model of ALS-associated neurodegeneration, which may be relevant for future clinical studies and interventions in ALS.

Introduction

- Familial (genetic) ALS accounts for ~10% of all ALS cases, with mutations in FUS accounting for ~4-5% of FALS cases.
- Victims of ALS display loss of muscle mass, increased frailty, loss of mobility, and eventually death.
- Currently ALS has no definitive treatment in addition to being ultimately fatal, making the study of ALS all the more urgent and important.
- Steve Gleason, former New Orleans Saint and known ALS patient, in a simply a few years, has gone from inciting the loudest recorded noise in the Superdome with his blocked punt all the way to a man confined to a wheelchair and deprived of his former stature.

- Knowing that FUS in itself is an RNA-binding protein, we hypothesized that disruption of its RNA binding ability by deletion of the RRM domain or by 4F-L mutations would reduce the toxicity of mutant FUS.
- We started by transfecting neuronal cells with FUS and corresponding FUS mutations. We then tested our hypothesis by creating transgenic lines with a deletion of the RRM domain in FUS entirely (RRM-D). We next narrowed our focus and created transgenic lines in which we mutated 4 conserved phenylalanine residues within the FUS RRM to leucine (known as 4F-L). Both the RRM-D and 4F-L lines were used in screens in which the FUS trans-gene was expressed in the fly eyes.

I. FUS Gene Model

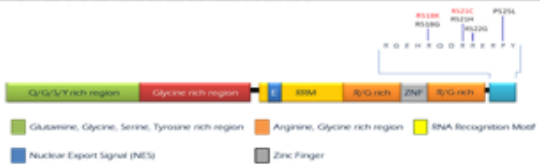

Figure 1: In 2009, ALS-causing mutations in the FUS gene were identified and led to a line of thinking that perhaps errors in RNA metabolism could be involved in ALS pathogenesis.

II. A *Drosophila* model of FUS
Lanson N A et al.

- Recently, our lab developed a *Drosophila melanogaster* (fruit fly) model as a highly useful system for studying FUS-induced proteinopathies such as ALS.
- Fly models of FUS recapitulate several key features of ALS, demonstrating pupal lethality and larval locomotion defects.

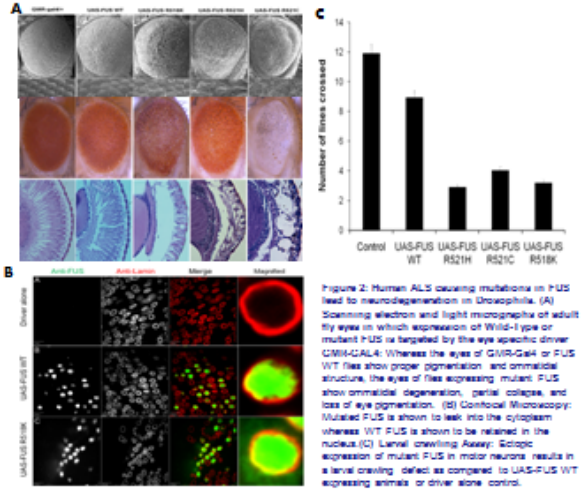

Figure 2: Human ALS causing mutations in FUS lead to neurodegeneration in Drosophila. (A) Scanning electron and light micrographs of adult fly eyes in which expression of Wild-Type or mutant FUS is targeted by the eye specific driver GMR-GAL4: Whereas the eyes of GMR-Gal4 or FUS WT flies show proper pigmentation and ommatidial structure, the eyes of flies expressing mutant FUS show ommatidial degeneration, partial collapse, and loss of eye pigmentation. (B) Confocal Microscopy: Mutated FUS is shown to leak into the cytoplasm whereas WT FUS is shown to be retained in the nucleus.(C) Larval crawling Assay: Ectopic expression of mutant FUS in motor neurons results in a larval crawling defect as compared to UAS-FUS WT expressing animals or driver alone control.

III. RNA Binding ability is essential for FUS-related neurodegeneration.

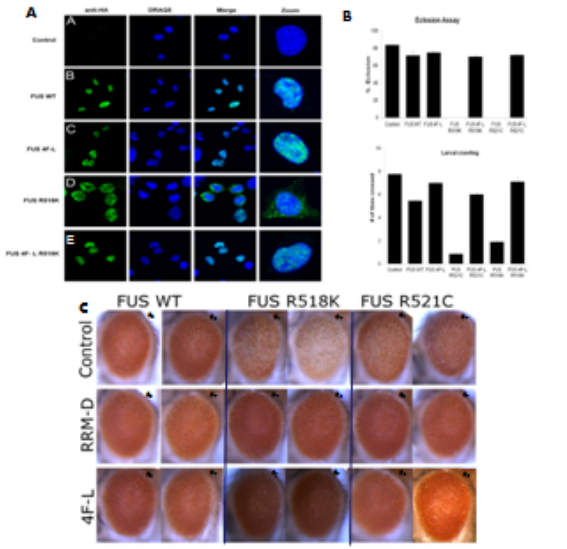

Figure 3: RNA-binding ability of FUS regulates toxicity and subcellular localization. (A) Confocal Imaging: In neuronal cells, WT FUS (B) is predominantly nuclear whereas FUS with ALS-linked mutation (D) is redistributed into the cytoplasm. RNA-binding incompetent FUS along with an ALS-linked mutation (E) is localized in the nucleus. (B) Behavioral Assays: When FUS was targeted by the motor-neuron specific driver (OK-gal4), we observed greater lethality among pupae with an ALS-linked mutation as opposed to normal eclosion in WT or RNA-binding deficient FUS. Similarly, we observed that expression of mutant FUS in motor neurons results in a larval crawling defect as compared to normal locomotion from FUS WT and non-transgenic controls. Interestingly RNA-binding incompetent larvae also displayed normal locomotion. (C) Light Micrographs of Crossed transgenic Fly lines: Expressing R518K or R521C mutations in fly eyes led to external eye degeneration. However, blocking RNA binding by deleting the RRM domain or by 4F-L mutation rescues the degenerative phenotype.

Conclusions

- Disrupting the RRMDomain by way of deletion or by 4F-L mutations does indeed seem to significantly rescue phenotype in mutated FUS fly eyes.
- For further research, we want to express RNA-binding deficient FUS mutations in motor neurons of flies and assess neurodegeneration with respect to motility and larval crawling ability.
- We would also like to further investigate the link between subcellular localization of FUS and its toxicity, a point of interest which showed up in these experiments.

- Lanson, N. A., et al, 2011. A *Drosophila* model of FUS-related neurodegeneration reveals genetic interaction between FUS and TDP-43. Human Molecular Genetics. 20, 2510- 2523.
- Lanson, N.A., Pandey, U.B., FUS related proteinopathies: Lessons from animal models, Brain Res. [2012], doi:10.1016.2012.01.039

- Acknowledgements: This work was supported by the ALS association and the Robert Packard Center for ALS at Johns Hopkins Medical Center. We would also like to thank the Louisiana Vaccine Center and LSU Health Sciences Center for their generous support.

Example of a better poster

LOUISIANA GENE THERAPY RESEARCH CONSORTIUM

AXIN2 Gene Instability In Colon Cancer

Summer Student (you), People who helped you, mentor

Mentor's department and University

LSU Health Sciences Center

Abstract

Colon cancer is one of the most prevalent and fatal cancers in the world. In the United States, 10% of all cancer patients have colon cancer. The disease begins when adenomatous polyps, fleshy growths that line up on the inside of the colon, become cancerous. Colonoscopy is often performed to detect these polyps. Regular testing after the age of 40 can drastically reduce the risk of developing colon cancer.

The AXIN2 gene, located in the region of 17q23-q25, is a gene of interest due to its interaction with the Adenomatous polyposis coli (APC) gene in the Wnt signaling pathway and its association with colon cancer with defective mismatch repair. Mutations in the Adenomatous polyposis coli (APC) gene have been found in about 85% of colon cancer patients. However, not much is currently know about the role of AXIN2 in colon cancer development. By conducting research on AXIN2, researchers are hoping that this gene may assist in distinguishing different subgroups of colon cancer. For this project, we analyzed two colon cancer cells lines to determine their karyotypic differences and for any 17q23-q25 region abnormalities.

The majority of the metaphase cells from both of the colon cancer cell lines analyzed were aneuploid, with one cell line (SW480) having a dramatically higher number of chromosomes reaching hypertetraploidy (103 chromosomes). In addition, the SW480 cell line contained some metaphase cells with an extra copy of chromosome 17 with amplification of the 17q23-25 region. This is the gene location of AXIN2, indicating the possibility of AXIN2 over-expression leading to the colon cancer in this cell line.

Introduction

The colon is the last portion of the large intestine, which also includes the rectum. Colorectal cancer (CRC), also known as colon cancer, is the third most common cancer in the world and the second most fatal cancer in the Western hemisphere. It is reported that approximately 655,000 people worldwide die from this disease every year. It usually arises from adenomatous polyps that line the inside of the colon. Mutations in certain genes are have been associated with this disease.

One significant gene known to cause CRC is the adenomatous polyposis coli gene (APC). The APC gene is located on the chromosome 5 between positions 21 and 22. Its normal function is to provide instructions for the creation of the APC protein, which helps control how and when a cell should divide. Mutations in this tumor suppressor gene can cause CRC, gastric (stomach) cancer, and Turcot syndrome. Approximately 85% of the people who have colon cancer have a mutation in the APC gene. If a person inherits just one defective copy of the gene from one of their parents, then he or she is almost guaranteed that they will develop colon cancer by the age of 40.

A gene that the APC interacts with is the relatively unknown AXIN2 gene, the focus of this project. Located on chromosome 17 between positions 23 and 24, this gene's protein, Axin2, is presumably very important in the regulation of beta-catenin, which is also a function of the APC gene. Since the APC gene and AXIN2 gene interact in the same pathway, it is believed that a mutation to either gene can affect the other gene. About 30% of the people with colon cancer with defective mismatch repair (the mechanism to correct DNA replication errors) have a mutated AXIN2 gene. The region containing the gene shows loss of heterozygosity in breast cancer, neuroblastoma, and other cancers and tumors. Deletions or mutations in this gene can result in truncated proteins which are most likely inactive. There is a possibility that somatic inactivating mutations in AXIN2 can deregulate beta catenin, and therefore, AXIN2 may be tumor suppressor gene.

Colon Cancer Symptoms

- Constipation
- Thin stool
- Hematochezia (Blood in stool)
- Vomiting
- Diarrhea
- Unexplained Weight loss
- Stomach cramps

Figure 1

The AXIN2 gene is located on Chromosome 17 on the q arm (long arm) between positions 23 and 24. The gene spans about 35 kbp and 843 amino acids.

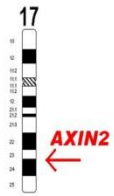

Figure 2

The Four Stages of Colon Cancer

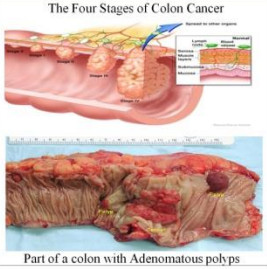

Part of a colon with Adenomatous polyps

Figure 3

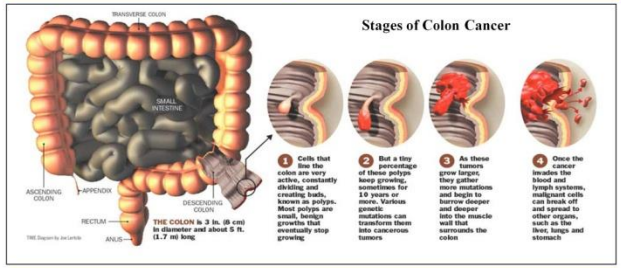

Figure 4

G-banded Metaphases From Colon Cancer Cell lines

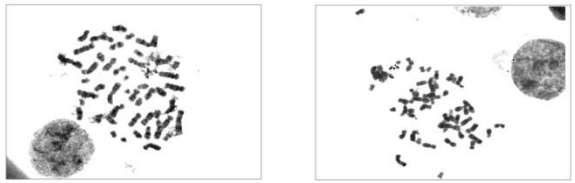

Sw48 Cell | Sw480 Cell

Methods and Materials

Samples and Culture Conditions:

Two colon cancer lines were obtained from human patients. The Sw48 cell line was obtained from an 82 year old female and the SW480 cell line was obtained from a 50 year old male. The cells were grown in DMEM with 10% Fetal Bovine Serum (FBS) and 1% penicillin under normal culturing conditions.

Chromosome Preparation:

For solid staining and G-banding, cells were harvested in exponential phase, incubated with colcemid, treated with a KCL hypotonic, and fixed two times with methanol and acetic acid. For solid staining, the cells were dropped onto slides and stained with Giemsa. For G-banding, the cells were dropped onto slides, followed by a short incubation in a trypsin solution prior to staining with Giemsa.

Results

The table to the right shows the frequency of different ploidies in the Sw48 and Sw480 colon cancer cell line.

Ploidy of Human Colon Cancer Cell Lines

	Sw48	Sw480
Total # of cells analyzed	35	20
Diploidy = 46 (Normal #) (%)	2 (6%)	0 (0%)
Hyperdiploidy 47-57 (%)	33 (94%)	6 (30%)
Hypotriploidy 58-68 (%)	0 (0%)	8 (40%)
Triploidy = 69 (%)	0 (0%)	0 (0%)
Hypertriploidy 70-80 (%)	0 (0%)	1 (5%)
Hypotetraploidy 81-91 (%)	0 (0%)	4 (20%)
Tetraploidy 92 (%)	0 (0%)	0 (0%)
Hypertetraploidy 93-103 (%)	0 (0%)	1 (5%)

G-Banded Karyotypes Representative of Colon Cancer Cell lines. The Red Arrows indicate abnormalities.

Sw48 Cell

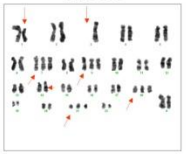

49, XX, Del (1), (p31), -3, +7, +9, inv (14) (q11q22), +18, +21

Sw480 Cell

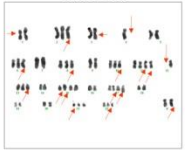

57, X-Y, +der X, iso (1q), +2, iso (3q), -4,+6, +8, +10,+11,+11, -12, +13, +15, +17, +add (17) (q23), +21, +22

Conclusions and Future Directions

When compared to normal human diploid cells, the majority of the cells from the Sw48 cell line were hyperdiploids ranging from a total of 47 to 57 chromosomes per cell, while the Sw480 cell line had a wide range of total chromosome number ranging from hyperdiploidy to hypertetraploidy (up to 103 chromosomes). Our results had many similarities with published literature on these cell lines. For example, both previously published and our analysis of sw40 showed the presence of some diploid cells as well as some hyperdiploidy, with an extra chromosome 7 in common.

The sw480 cell line was much more unstable in both studies, with common abnormalities including a missing Y, an extra X abnormal X chromosome, isochromosome 3q, and trisomy 13, 21, and 22. The previous report found one extra chromosome 17. However, our results show four 17 chromosomes, with one of them containing additional genetic material at the q23-qter, the critical region of the AXIN2 gene. Fluorescence *in situ* hybridization (FISH), RNA, and protein analyses should be preformed to determine the extent of AXIN2 amplification in the Sw480 cell line.

Due to the nature of these immortalized cell lines, chromosome abnormalities are acquired with increased cell proliferation. *In vitro* studies such as this one can help to gives an idea of what can occur *in vivo*. More cancer cell lines should be analyzed in order to find genetic differences between the various types of colon cancer.

Expression of *Irf-7* in Plasmacytoid Dendritic Cells is Limited Following Neonatal Respiratory Syncytial Virus Infection

Names
Affiliations

Abstract

Nearly all infants are infected with respiratory syncytial virus (RSV) by two years of age. In infants, RSV is the major cause of bronchiolitis and infants who acquire severe RSV bronchiolitis are at risk of developing asthma. Immune protection is incomplete and reinfection is common throughout life. In otherwise healthy adults, RSV infection usually induces mild upper respiratory tract disease. The mechanisms whereby RSV induces severe disease in infants are largely unknown.

We previously found that neonatal, unlike adult, mice fail to induce appropriate antiviral defenses. In particular, type I interferons are not produced in response to RSV infection. As type I interferons are mainly produced by plasmacytoid dendritic cells (pDCs) via interferon regulatory factor 7 (IRF-7: a transcription factor), we hypothesized that neonatal pDCs in response to RSV infection express less *Irf-7* than adults.

To test this hypothesis, we infected neonatal mice (5d old) and adult mice (7-8wks old) with RSV and purified pDCs from the lung 24h post infection. We then isolated total RNA from the purified pDCs and reverse transcribed the RNA to produce cDNA. Real time PCR was performed with the resulting cDNA to quantify the relative amount of *Irf-7* in neonatal and adult pDCs.

We found that pulmonary pDCs from naïve neonates express seven fold less *Irf-7* than pDCs from adults. When infected with RSV, expression of *Irf-7* in pulmonary pDCs from both neonates and adults increased; however, neonatal pDCs expressed significantly less *Irf-7* than adults. These data indicate that the muted induction of Irf-7 expression in pDCs may play a role in RSV pathogenesis in neonates.

Introduction

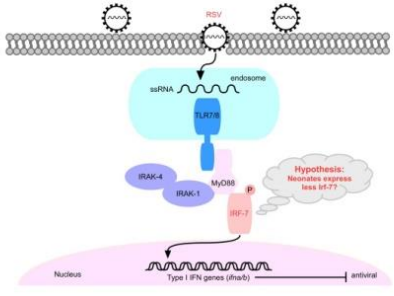

Fig1: RSV induces Type I IFN production in adult pDCs. RSV enters the cells and fuses with endosomal membrane releasing its genomic ssRNA. ssRNA is recognized by host TLR7/8 and induces a cascade of signaling events leading to the phosphorylation of IRF-7. Phosphorylated IRF-7 then translocates to the nucleus and promotes the expression of type I IFNs.

Methods

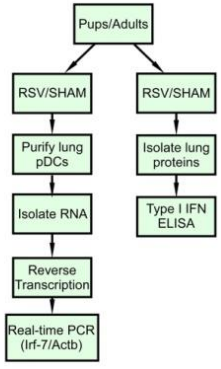

Fig 2: Schematic of the experimental design. Five day old pups or 6-8 wks old adults were infected with RSV or sham infected with media. At one day post infection, total protein was isolated from the lungs of half of the mice. Type I IFNs were measured in the isolated protein using ELISA. The other half of the mice were used for lung pDC purification. RNA were isolated from these purified pDCs and reverse transcribed to cDNA. The resulting cDNA were subjected to real-time PCR to measure the expression of *Irf-7* in pDCs.

Purity of the Isolated pDCs

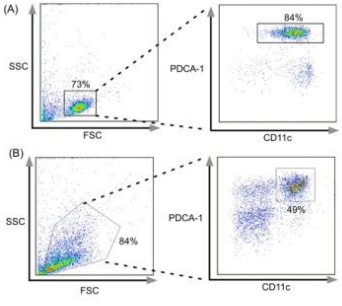

Fig 3: Purity of the isolated pDCs. Five day old pups and 6-8 wks old adults were infected with RSV. The pDCs were purified using gradient density centrifugation and magnetic bead selection. The resulting cells from the purification were then labeled with CD11c and PDCA-1 antibodies to identify pDCs. (A) Purified pDCs from adult lung. (B) Purified pDCs from neonatal lung.

Neonatal RSV Infection Induced Limited Expression of *Irf-7*

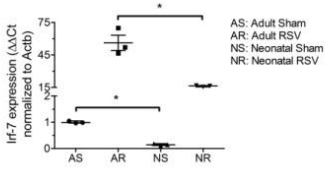

Fig 4: Relative expression of *Irf-7* in pulmonary pDCs. Five day old neonates or 6-8 wks old adults were infected with RSV. pDCs were purified at 1 day post infection; and the expression of *Irf-7* in these cells were quantified using real time PCR. NS: sham infected neonates; NR: RSV infected neonates; AS: sham infected adults; AR: RSV infected adults. *: $p<0.05$.

Neonatal RSV Infection Induced Limited Type I IFNs Response

	IFNα (ng/g lung protein)	IFNβ (ng/g lung protein)
NS	4.35 ± 0.78	5.57 ± 1.13
AS	3.77± 0.89	8.14 ± 2.31
NR	5.51± 1.02	11.8 ± 2.43*
AR	76.2 ± 11.2*#	42.3 ± 5.07*#

Fig 5: Type I IFNs in lung homogenates. Neonatal or adult mice were infected with RSV and total lung protein was isolated using T-Per (Pierce). IFNα and IFNβ were then measured using ELISA at 1 day post-infection. NS: sham infected neonates; NR: RSV infected neonates; AS: sham infected adults; AR: RSV infected adults. *: $p<0.05$; NR vs. NS or AR vs. AS; #: AR vs. NR.

Conclusions

- Neonatal pDCs express less *Irf-7* than adult pDCs at baseline.
- RSV infection induces *Irf-7* expression in both neonatal and adult pDCs; however, expression of *Irf-7* in pDCs from neonates is muted compared to adults.
- RSV infection induces limited amount of type I IFNs (IFNα and β) in neonates.
- The muted expression of *Irf-7* and resulting reduction in type I IFNs may play a role in neonatal RSV pathogenesis.

Acknowledgement

The project described was supported by LVC and Grant Number (5R01 AI090059) from NIAID. Its contents are solely the responsibility of the authors and do not necessarily represent the official views o NIAID/NIH.

"Prostate Cancer Genetics: How Informative is Your Family?"

Brianne Jones, Elisa Ledet and Diptasri Mandal.
Louisiana State University Health Sciences Center-New Orleans.

Introduction

- **In 2012, the American Cancer Society estimates that approximately 242,000 cases of prostate cancer will be diagnosed and approximately 28,000 men will die of prostate cancer in the U.S.**
- **The three most important risk factors for prostate cancer are age, race, and family history.**
  - Having a first degree relative with prostate cancer can double the risk of developing prostate cancer.
- **In the U,S., African American men have a 60% higher incidence rate than white men.**
- **Many genetic studies prostate cancer have been done; however, these studies were conducted on European cohorts and African Americans have been underrepresented.**
- **Due to disease and locus heterogeneity, few prostate cancer studies have been successful in consistently identifying a specific gene or set of genes responsible for causing prostate cancer.**
- **The objective of the present study was to compare how known prostate cancer families would perform in an idealized linkage scenario, under certain assumptions, versus experimental conditions.**
  - This illustrates the complexity of familial studies and prostate cancer genetics, and emphasizes the importance of careful family selection.

Recruitment

- **Prostate cancer families for this study were recruited from South Eastern and South Central Louisiana beginning in 2001.**
- **To be considered a high risk prostate cancer family, the family must meet at least one of the following criteria:**
  - Three or more affected first degree relatives present in the family.
  - Prostate cancer has occurred in three or more successive generations.
  - Two or more individuals diagnosed with prostate cancer at age 55 or younger.
- **Data was collected from the families including the number of affected individuals, the number of generations with prostate cancer, clinical information and the availability of DNA.**
- **From these African American families, two highly informative families (number of affected ≥ 6) and one less informative family (number of affected = 3) were selected.**

Methods: Simulation

- **SIMLINK software was used to perform a simulation study based on the pedigree structure of each family to assess how informative the given families would be for linkage analysis.**
- **Marker genotypes for genetic markers at different recombination fractions are simulated and maximum LOD scores for each recombination fraction are calculated.**
- **To demonstrate linkage two measures of information are used:**
  - The expected maximum LOD score
  - The probability that the max LOD score is greater than or equal to 3.0

Methods: Linkage Analyses

- **3 large high-risk families were selected for analyses**
  - 30 individuals included with 11 affected men, 11 currently unaffected men and 8 informative women.
- **Families were genotyped with Illumina Infinium II SNP HumanLinkage-12 panel**
- **Both parametric and non-parametric linkage analyses were performed with Merlin (v1.1.2)**

Family Data

Figure 1abc. Pedigrees for a subset of high risk African American prostate cancer families.

a. Family 1- Highly informative

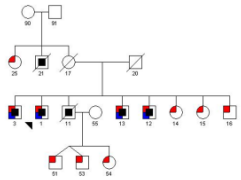

c. Family 3- Less informative

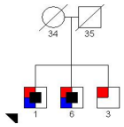

b. Family 2- Highly informative

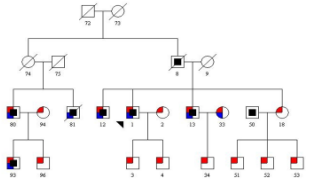

Table 1. Characteristics of the African American prostate cancer pedigrees selected for simulation and linkage analyses

	Total no. of available genotypes	Total no. of affected genotypes	No. of Affected per family	Average age at diagnosis	Median PSA (ng/ul)	Average Gleason Score
All families (n= 15)	129	45	4.3 (avg)	60.8	6.2	6.3
Family Subset (n= 3)	30	11	5.3 (avg)	60.9	8.6	6.7
Family 1	11	4	6	56.8	5.25	7.25
Family 2	16	5	8	64.3	8.6	6
Family 3	3	2	2	N/A	124	7.5

Results: Simulation

Table 2. Maximum LOD-scores estimated on individual prostate cancer families using an eight-allele marker.

Family IDs	No. of family members	*Maximum LOD-scores*					
		θ= 0.00	**θ= 0.01**	**θ= 0.05**	**θ= 0.10**	**θ= 0.20**	**θ= 0.50**
Family 1	18	0.575	0.175	0.568	0.580	0.348	0.189
Family 2	24	1.135	1.118	0.186	1.150	1.128	0.190
Family 3	6	0.227	0.179	0.198	0.227	0.232	0.232

Table 3. Summed maximum LOD-scores estimated on prostate cancer families using an eight-allele marker.

Summed maximum LOD-scores					
θ= 0.00	**θ= 0.01**	**θ= 0.05**	**θ= 0.10**	**θ= 0.20**	**θ= 0.50**
0.656	0.958	1.250	0.436	0.436	0.262

Results: Linkage Analyses

Chromosome	cM	Left flanking SNP (bp)	Right flanking SNP (bp)	NPL	Dominant HLOD	Recessive HLOD
6	13.39	**rs190129** (3663360)	**rs2025267** (4103521)	0.82	**1.56**	0.51
2	117.9	**rs1022298** (103601066)	**rs1026220** (104962840)	0.84	**1.36**	0.98
2	141.16	**rs2016244** (125989202)	**rs1484448** (126678671)	0.34	**1.10**	0.48
13	19.3	**rs1974047** (18602915)	**rs1334958** (18439910)	0.91	**1.04**	1.03
14	633.3	**rs961700** (67401190)	**rs927221** (67911913)	0.63	0.73	**0.97**
14	45.84	**rs1947393** (49052346)	**rs1349750** (49112518)	0.74	0.74	**0.96**

Table 4. Summary of non-parametric and parametric linkage analyses.

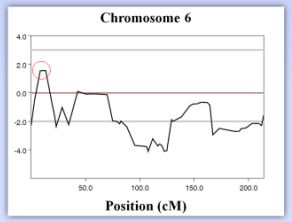

Figure 2. Individual HLOD plot for chromosome 6 in 3 African American prostate cancer families. Linkage results at 6p25 with an HLOD score of 1.56 under the dominant model using Merlin (v1.1.2).

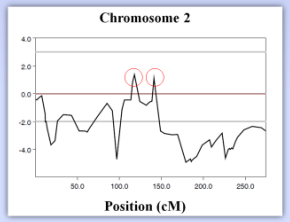

Figure 3. Individual HLOD plot for chromosome 2 in 3 African American prostate cancer families. Linkage results at 2q12 and 2q14 with an HLOD score of 1.36 and 1.10 respectively under the dominant model using Merlin (v1.1.2).

Conclusions

- **After simulation with Simlink, based on the maximum possible LOD scores, we demonstrated that the best families for linkage analysis had a large number of available genotypes, and affected family members in more than one generation.**
  - There were parameter limitations inherent in Simlink which make this simulation less accurate for this situation; however, this simulation is still important in assessing how much information individual families contribute to linkage analyses.
  - A second simulation, conducted with Merlin, produced a maximum summed LOD score 1.84 for these 3 families.
- **The 3 highest linkage peaks in 3 families were observed at 6p25 (HLOD= 1.56), 2q12 (HLOD= 1.36), and 2q14 (HLOD= 1.10).**
  - These peaks are below the genomewide threshold of significance, but indicate that linkage may be present.
  - Also, 6p25 has been previously reported as a possible prostate cancer susceptibility locus.
- **These results demonstrate the necessity of ascertaining a large collection of highly informative families in order to effectively conduct a linkage study.**

References:

Howlader N, Noone AM, Krapcho M, Neyman N, Aminou R, Altekruse SF, Kosary CL, Ruhl J, Tatalovich Z, Cho H, Mariotto A, Eisner MP, Lewis DR, Chen HS, Feuer EJ, Cronin KA (eds).*SEER Cancer Statistics Review, 1975-2009 (Vintage 2009 Populations)*, National Cancer Institute. Bethesda, MD, http://seer.cancer.gov/csr/1975_2009_pops09/, based on November 2011 SEER data submission, posted to the SEER web site, 2012.

Abecasis GR, Cherny SS, Cookson WO and Cardon LR (2002). Merlin-rapid analysis of dense genetic maps using sparse gene flow trees. *Nat Genet* **30**:97-101.

Boehnke M. and Ploughman LM. SIMLINK: A Program for Estimating the Power of a Proposed Linkage Study by Computer Simulation. Version 4.12, April 2, 1997

Primate Femur Histomorphometry and Gene Expression: Effects of Chronic Alcohol Abuse on Bone

S. Frischhertz, D. Feng[1], C. Les[2], C. Pechey[2], R.W. Siggins[3], S. Nelson[4], G.J. Bagby[3,4], J. Dufour[5], P.E. Molina[3,4], M. Lopez[1]

[1]Laboratory for Equine and Comparative Orthopedic Research, School of Veterinary Medicine, Louisiana State University (LSU), Baton Rouge, LA, [2]Bone and Joint Center, Henry Ford Health System, Detroit, MI, [3]Department of Physiology, LSU Health Sciences Center, New Orleans, LA, [4]Comprehensive Alcohol Research Center, LSU Health Sciences Center, New Orleans, LA, [5]Tulane National Primate Research Center, Covington, LA

Introduction

- Problem: Alcohol abuse is a widely recognized health concern that negatively impacts many organ systems.
  - Chronic alcohol consumption leads to secondary osteoporosis with decreases in bone formation, bone mass, and bone mineral density.
  - Specific mechanisms must be better understood to optimize therapeutic intervention.
- Objective: This study was designed to relate the specific histomorphometric changes with osteoclastic and osteoblastic gene expression alterations in a primate model of alcohol abuse.

Materials

- Seven 3-4 year old male rhesus macaques: 19 months of treatment via indwelling intra-gastric tube
  - 3 primates received alcohol diet
    - 13-14 kg/week (30% W/V in water)
  - 4 primates received isocaloric sucrose diet
- Proximal femora were harvested for analysis
  - *Left femur*: qRT-PCR mRNA analysis
    - Isolated greater trochanter
    - Stored in RNAlater (Qiagen)
  - *Right femur*: Histomorphometry
    - Embedded in PMMA
    - Coronal sections
    - Toluidine blue stain

Histomorphometry: Methods

- Two methods used for analysis:
  - *Manual*: Merz Grid
    - Ocular grid over bone
    - Manual assessments
    - Calculations
  - *Semi-automated*: ImagePro v.5.01
    - Digital bone images (Leica DFC480)
    - Manual surface tracing
    - Software length and area calculations

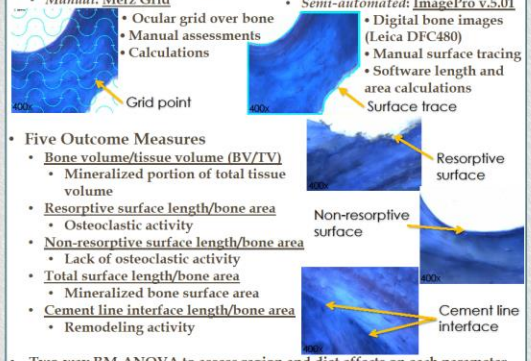

- Five Outcome Measures
  - Bone volume/tissue volume (BV/TV)
    - Mineralized portion of total tissue volume
  - Resorptive surface length/bone area
    - Osteoclastic activity
  - Non-resorptive surface length/bone area
    - Lack of osteoclastic activity
  - Total surface length/bone area
    - Mineralized bone surface area
  - Cement line interface length/bone area
    - Remodeling activity
- Two-way RM-ANOVA to assess region and diet effects on each parameter ($p<0.05$).

Bone Regions

- 16 bone regions examined for each parameter: 945 individual measurements
- 9 Cancellous regions
  - Femoral Head
    - Inferolateral (a), Superolateral (b)
  - Femoral Neck
    - Inferomedial (c), Superolateral (d)
  - Proximal Greater Trochanter
    - Proximal (e), Lateral (f), Mid/Medial (g)
  - Distal Greater Trochanter
    - Medial (h), Lateral (i)

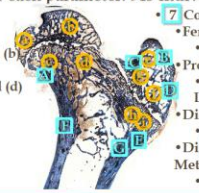

- 7 Cortical regions
  - Femoral Neck
    - Inferior (A)
  - Proximal Greater Trochanter
    - Proximal (B), Medial (C), Lateral (D)
  - Distal Greater Trochanter
    - Lateral (E)
  - Distal Portion of the Proximal Metaphysis
    - Medial (F), Lateral (G)

Histomorphometry: Results

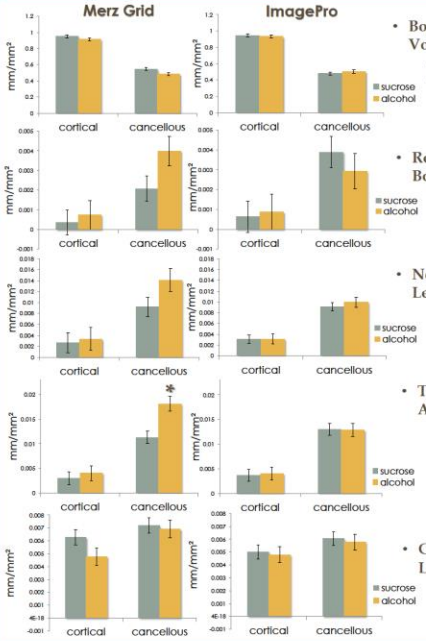

- Bone Volume/Tissue Volume
  - Little change
  - Possible ↓ in mineralized portion of total tissue volume
- Resorptive Surface Length/ Bone Area
  - Mixed results for osteoclastic activity
- Non-resorptive Surface Length/Bone Area
  - ↑ areas without osteoclastic activity
- Total Surface Length/Bone Area
  - * Significant ↑ in cancellous bone of the alcohol group using Merz grid data
- Cement Line Interface Length/Bone Area
  - ↓ remodeling activity

RT-qPCR: Methods and Results

- Total RNA isolated from the left greater trochanters
- Messenger RNA levels of osteoblastic and osteoclastic target genes quantified with RT-qPCR using SYBRGreen technology

- Trends associated with alcohol consumption:
  - ↓ expression of osteoblastic genes
  - Altered expression of osteoclastic genes
    - Activation: overall ↑
    - Migration: ↑
    - Resorption: possible net ↑

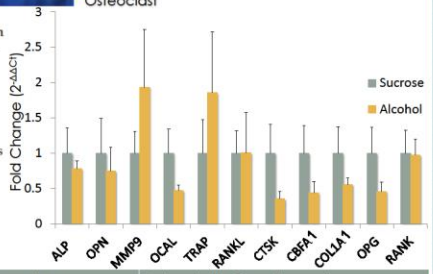

Osteoblastic Gene Expression	Osteoclastic Gene Expression
Runt related transcription factor 2 (CBFA1) ↓	Cathepsin K (CTSK) ↓
Osteocalcin (OCAL) ↓	Matrix Metalloproteinase 9 (MMP9) ↑
Osteopontin (OPN) ↓	Tartrate resistant acid phosphatase (TRAP) ↑
Osteoprotegerin (OPG) ↓	Receptor activator of nuclear factor kappa beta (RANK) ↓
Collagen 1 alpha 1 (COL1A1) ↓	RANK ligand (RANKL) (no change)
Alkaline phosphatase (ALP) ↓	

Conclusions

- This study was limited by sample size, but the preliminary results suggest that disruption of bone homeostasis at the mRNA level by chronic alcohol exposure contributes to the specific histomorphometric alterations of secondary osteoporosis.
- While larger studies are warranted to further examine the effects of alcohol ingestion on bone remodeling, potential gene targets for treatment of patients suffering from the homeostatic bone alterations due to alcoholism are suggested by these study results.
  - Treatments reversing this ↓ osteoblastic and ↑ osteoclastic activity may benefit alcoholic patients suffering from secondary osteoporosis. Monoclonal antibody binding RANKL (Denosumab) may reverse the effects of ↓ OPG and recombinant parathyroid hormone (teriparatide) may help to ↑ lost osteoblastic function (for high risk cases). Bisphophonates may also be effective in reducing osteoclastic activity.

Acknowledgements

- Thank you to Carmel Fargason and Laura Kelly for their efforts in making this project a success.

This research was supported by grants 1T35AA021097, AA009803, and AA020312 from the National Institute of Alcohol Abuse and Alcoholism.

Influenza Vaccination Program Requirements of Healthcare Personnel in Louisiana Hospitals

names

LSUHSC-NOLA, Department of Pediatrics, Division of Infectious Diseases and Children's Hospital, New Orleans

Introduction

- Influenza virus causes 24,000 annual deaths in the U.S. Every year 450,000 to 900,000 Louisiana residents are infected and 800 die.
- To prevent high morbidity and mortality, annual vaccination of patients and healthcare personnel (HCP) is recommended. Yet, the vaccination coverage of U.S. HCP in 2010 was only 60%.
- In response, the Centers for Disease Control and Prevention (CDC) is demanding that vaccination rates improve to 90% by 2020, and various Medical Societies are recommending mandatory vaccination programs (i.e., requirement for employment).
- To improve influenza vaccination coverage of HCP in Louisiana hospitals we must first understand what is being done, what is effective and what is ineffective.

Objectives

1. To determine influenza vaccination requirements and policies among hospitals in Louisiana, including the prevalence of mandatory requirements and consequences for declination
2. To correlate specific requirements with vaccination rates achieved, and to identify interventions that may increase vaccination rates

Methods

- A survey was sent to all 256 hospitals in Louisiana (under 193 organizations) identified in the Directory of the Louisiana Hospital Association.
- The survey contained questions on type of hospital, patient population served, components of the vaccination program and their estimated vaccination rate.
- Data was inputted into an Excel sheet and analyzed for components that influenced vaccination rates.
- Univariant analysis of categorical data compared the median vaccination rate between hospitals with or without a specific variable using the non-parametric Mann-Whitney test.
- The effect of continuous variables on the vaccination rate was analyzed with regression analysis using the non-parametric Spearman r.
- A p Value of <0.05 was considered significant.

Results: Hospitals Responding

- In the first 4 weeks, 49 (25%) of the 193 administrations responded with a statewide distribution (Figure 1).

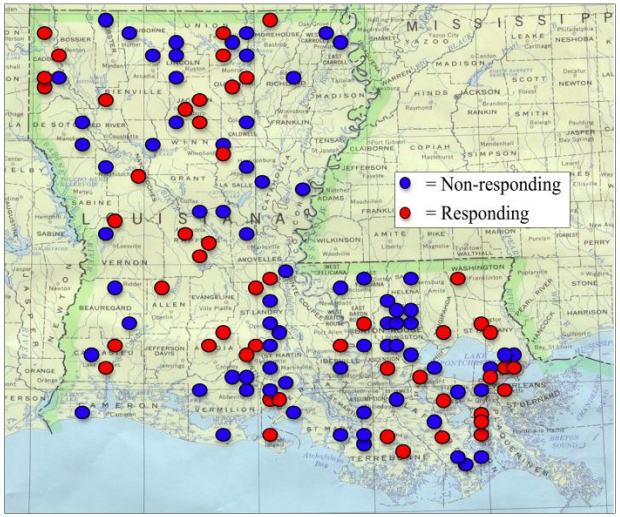

Results: Main Responses

- Most hospitals were private for profit (51%), private non-profit (35%), and public (14%); 22% were teaching and 51% were accredited by The Joint Commission.
- The median number of beds was 60 with a range of 10 – 800.
- All hospitals had a flu vaccination program; 33% had voluntary vaccination and 67% required a formal declination. No hospital demanded vaccination as a requirement of employment.
- All hospitals offered free vaccines; 27% met all CDC recommended activities for vaccination but 73% did not meet all CDC recommendations.
- 24% of hospitals enforced consequences to HCP declining vaccination while 76% had no consequences; the most common consequence was a requirement to wear a mask on patient contact.
- The median vaccination rate reported by the responding hospitals was 61%, with a range from 12 - 98%.

Results: Correlates of Vaccination

Factors Positively Associated with Vaccination Rates

Survey Questions		No. Responses	%	Not Present	Present	Ratio	p Value
				Median (25%, 75%)			
Hospital Type							
	Private	18	37	55 (45, 72)	73 (58, 84)	1.33	0.02
	Acute Care	28	58	50 (45, 72)	70 (57, 81)	1.40	0.02
High-Risk Patient Type							
	Children	29	59	50 (45, 71)	70 (56, 85)	1.40	0.02
	Pregnant Women	23	47	51 (45, 71)	72 (60, 85)	1.41	0.004
	Intensive Care	26	53	50 (42, 70)	71 (57, 85)	1.42	0.006
Number of Beds							
	0 - 99	26	53		50 (45, 71)	0.694	0.0006
	100 - 299	12	24		70 (56, 80)	1.186	
	≥ 300	8	16		85 (61, 92)	1.466	
Vaccination Program							
	Voluntary	16	33	71 (52, 85)	52 (40, 57)	0.73	0.001
	Declination Required	33	67	52 (40, 57)	71 (52, 85)	1.37	0.001
Vaccine Administration							
	Common areas	31	63	48 (37, 52)	70 (59, 83)	1.46	0.001
	Nights/Weekends	38	78	50 (35, 60)	70 (53, 84)	1.40	0.006
Program Promotions							
	Fliers	37	76	43 (33, 56)	69 (55, 80)	1.60	0.005
	Email	34	69	50 (45, 71)	66 (54, 84)	1.32	0.05
Consequences upon Declination							
	None	37	76	86 (82, 93)	55 (45, 70)	0.64	0.0001
	Some consequence	12	24	55 (45, 70)	86 (82, 93)	1.56	0.0001
	Wear mask	10	20	56 (46, 70)	89 (85, 94)	1.59	0.0001

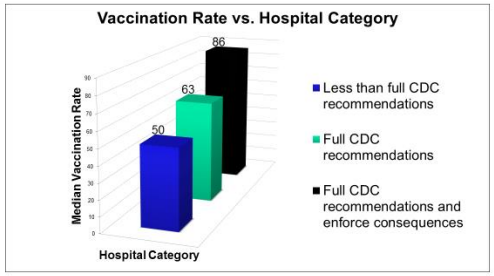

Conclusions

- Preliminary results demonstrate large variability among influenza vaccination programs in Louisiana hospitals. No hospital required vaccination as a condition of employment.
- Hospitals that impose consequences for vaccine declination have a higher vaccination rate than hospitals without consequences.
- Our findings suggest that to reach the goal of 90% vaccination rate by 2020, programs with consequences for declination (e.g. wearing a mask) must be enforced.
- These findings have important public health implications.

Lysyl oxidase inhibition in the volume overloaded heart prevents adverse collagen remodeling, apoptosis, and cardiac dysfunction

M.C. El Hajj, T.G. Voloshenyuk, M.A. Claudino, J.M. Bradley, and J.D. Gardner

LSU Health Sciences Center, Department of Physiology, New Orleans

Abstract

Heart failure is the most prevalent and costly disease in the U.S. Our goal was to determine if the over-activation of lysyl oxidase (LOX), a collagen cross-linking enzyme, accelerates cardiac disease and failure. LOX is elevated in human failing hearts, but it is not known if LOX plays a causative role in disease. Using the aortocaval fistula (ACF) rat surgical model of volume overload, we assessed the role of LOX activity in progression of heart failure over 14 wks. LOX activity was inhibited by beta-aminopropionitrile (BAPN; 100 mg/kg/d) at 2 wks post-surgery. Echocardiography was used to evaluate cardiac function and progression of LV remodeling. LOX expression and activity, collagen content, and cross-linking were determined in LV samples. Fixed sections of mid-LV were assessed for apoptosis by TUNEL. ACF surgery caused significant ventricular dilatation (43% increase) and dysfunction (26% decreased, %FS). LOX protein expression was increased (65%) with concomitant increases in LOX activity. These increases in LOX were associated with significantly elevated collagen concentration, cross-linking, and type I/III (not shown). LOX inhibition prevented ACF-induced changes in LV collagen, and led to maintenance of systolic function. LOX inhibition also attenuated LV dilatation and prevented apoptosis, but did not reduce LV hypertrophy. These data indicate that LOX inhibition is cardioprotective in the volume overloaded heart.

Methodology

Rodent Model of Congestive Heart Failure: Chronic volume overload was surgical created in adult male Sprague-Dawley rats. A ventral laparotomy was performed on anesthetized rats exposing the abdominal aorta and vena cava. Using an 18 gauge needle, a shunt is created between the aorta and vena cava producing volume overload (aortocaval fistula; ACF).

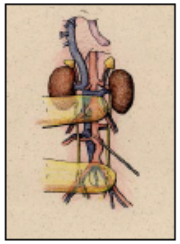

Assessment of Cardiac Function: In vivo ventricular dimensions and function were assessed temporally in sedated (Isoflurane 1.5%) rats by ultrasound echocardiogram (Visualsonics VEVO 770).

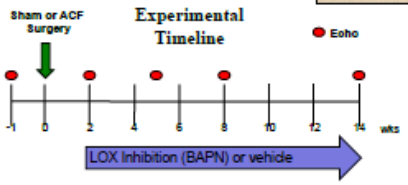

Cardiac LOX Protein Expression and Activity: Protein expression was measured in left ventricular homogenates by Western blot. Cardiac LOX enzymatic activity was assessed using an adaptation of the fluorometric technique described by Palamakumbura and Trackman.

Collagen Concentration and Cross-linking: Left ventricular collagen concentration was measured by hydroxyproline assay. LOX dependent collagen cross-linking was determined in the same hydrolyzed LV sample by commercial ELISA for pyridinoline (Quidel). Pyridinoline is a key component of the collagen cross-link that is formed by LOX.

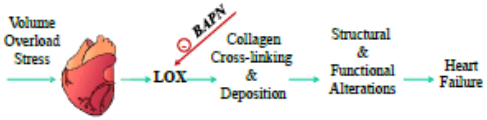

Results

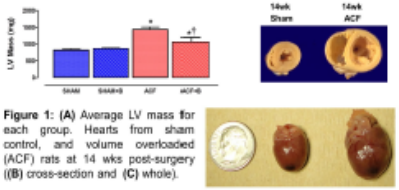

Figure 1: **(A)** Average LV mass for each group. Hearts from sham control, and volume overloaded (ACF) rats at 14 wks post-surgery (**(B)** cross-section and **(C)** whole).

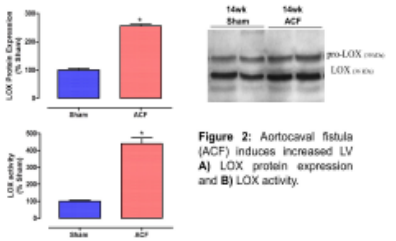

Figure 2: Aortocaval fistula (ACF) induces increased LV **A)** LOX protein expression and **B)** LOX activity.

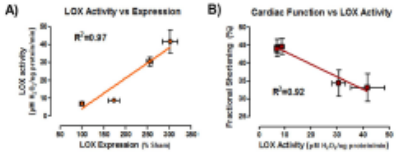

Figure 3: A) Increased LOX expression correlates positively to increased LOX activity. B) Negative correlation between LOX activity and systolic function.

Echocardiography

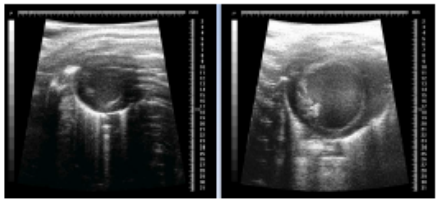

Sham **ACF**

Figure 4: Example B-mode ultrasound echocardiography images from SHAM and volume overloaded (ACF) rats. Echo was used to assess left ventricular dimensional and functional changes following surgery.

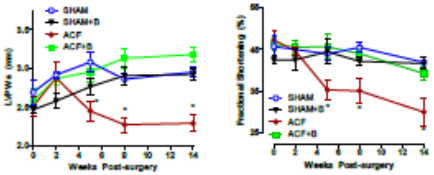

Figure 5: LOX inhibition with BAPN (100 mg/kg/d i.p.) initiated at 2 wks post-surgery prevented ventricular wall thinning (left; PWs = posterior wall at systole) and cardiac dysfunction (right).

Collagen

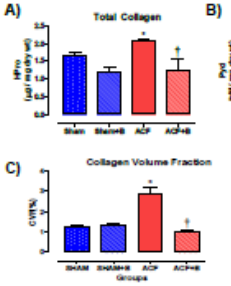

Figure 6: A) Total collagen content (hydroxyproline), B) LOX-dependent cross-linking (pyridinoline), and C) collagen volume fraction (Picrosirius Red) were increased in the ACF group compared to SHAM. LOX inhibition attenuated the volume overload-induced increases in collagen. ($p<0.05$; *vs. Sham; †vs. 14wk ACF+BAPN; n=5 to 8/group).

Apoptosis

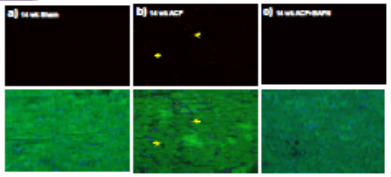

Figure 7: LOX inhibition (BAPN) prevented apoptosis in the ACF stressed rat heart. TUNEL assay was performed on fixed mid-left ventricular sections. Sections were then counterstained with Hoechst (nuclei) and Titin (cardiomyocytes). Top: TUNEL staining of apoptotic cells (red); Bottom: merge of TUNEL (red), nuclei (blue) and cardiomyocytes (green).

Conclusions

- Volume overload increased LV LOX activity and expression.
- Inhibition of LOX activity attenuated LV hypertrophy and prevented cardiac dysfunction and wall thinning.
- Inhibition of LOX activity prevented fibrosis and cardiomyocyte apoptosis.

Acknowledgments

This study was supported by the NIH/NCRR #P20RR016456 (D. Kapusta) and the American Heart Association Greater Southeast Affiliate #11GRNT7700002 (jdg). We also thank Conni Corri for her technical expertise.

Summer Research Internship Poster Day Thursday, July 27th, 2017

- 1st floor lobby of Medical Education Building (MEB), Lecture Room B, 1900 Perdido St., NO, LA 70112

8:00 am-9:00 am	Put up your poster
9:00 am-10:00 am	Interns and judges only
10:00 am-11:00 am	Open to the public
11:00 am- 12:00 noon	Awards ceremony, open to the public in MEB Lecture Room B